

Coupling finite element method and molecular dynamics for plane problem analysis

Byoungseon Jeon

Department of Applied Science, University of California, Davis, CA, 95616

I. INTRODUCTION

Continuum mechanics and atomistic analysis have been developed in their own interest and history. Finite element method (FEM) is one of the standard tools in solid mechanics and structural analysis. Molecular dynamics (MD) is a favored method for atomic and molecular interactions. In order to extend the capacity of computational methods, there have been efforts to bridge both of the methods.

FEM is quite stable tool and multi-purpose method for the most of the solid mechanics. But it exists on the base of continuum and has pitfalls on some of nonlinear cases - discontinuous media, crack propagation, phase transition, and so forth. Those nonlinear problems cannot be handled in the manner of continuum method because the problem domains do not exist on continuum any more. MD can handle atomistic and molecular analysis but takes heavy computing resource for huge problem sets, especially of continuum scale. Therefore we suggest an idea here - basic nonlinear and discontinuous behavior will be investigated using MD. Most of structures which maintain linear elastic state can be considered as continuum while they still transfer phonon (stress wave) and keep inertia - FEM region will work as an elastic reservoir. If an appropriate scheme is applied at the interface of FEM and MD, we will be able to maintain the system characteristics and extract reasonable results.

Here, we are going to show how FEM and MD are built and how they are connected for specific problems. Using plane strain analysis with linear elastic constitutive law, a simple FEM program was developed. Also two-dimensional MD program was built using Lennard-Jones (LJ) and embedded atom method (EAM) potentials. There could be numerous ways to bridge FEM and MD, but we afford one of the simple ways which address physical meanings.

II. FINITE ELEMENT METHOD WITH EXPLICIT TIME INTEGRATION

In the history of FEM development, implicit method has been favored. Considering connectivity of nodes and elements, solid structure can be represented by huge stiffness matrix. This method has been used in various fields of industrial engineering and plays an important role in computational analysis.

Explicit FEM was adopted in hydrodynamic problem and ballistic research - this method integrates stress wave and can solve the phenomena at high strain and high velocity re-

gion. Even though convergence, which is a basis of implicit method, is not available but explicit FEM was found to have brought enormous results under severe conditions: impact mechanics, terminal ballistics, and high strain rate behavior of materials.

Diverse methods and options are available on FEM itself, but we limit our approach into linear shape function, 4 point integration, plane strain, constant density, lumped mass matrix, linear elasticity and quadrilateral element.

A. Preprocessing

Besides of FEM solving, building computer-aided model is a critical issue. Including concurrent engineering, many commercial computer aided design (CAD) tools have been developed with various functions and interface. Using CAD model data, FEM mesh can be generated using those programs while simple geometry can be processed only for finite element analysis (FEA) - those procedure which produce meshes and nodes from conventional CAD model and simple geometry, are called as preprocessing. Effective mesh size and shape is quite important for FEM analysis and they are hot issues in those fields. Various study and algorithms have been developed for this objective but description of them is beyond of the current study.

Even though we are able to use commercial or free program for mesh generation, we need add-on feature - coupling particle and FEM mesh. Therefore we need to develop a tool which can arrange particle and mesh data effectively. Using PYTHON script language and graphic library like Tkinter, we developed simple program which can draw quad and generate mesh and particle.

B. Development of plane strain FEA

Below sections show how to build explicit FEM code. For detailed descriptions, readers can refer standard FEM textbook¹. Basic approach is Updated Lagrangian which configures current state as a reference.

1. Simulation loop

Program gets started and reads initial data of nodes and element components. As time loop begins, mass routine is run at first. Element geometry is mapped into unit coordinate(ξ, η) and mapping parameter is stored as Jacobian. Using Gauss quadrature, nodal mass is estimated. Also Jacobian term and gradient of shape function on every Gauss point are stored. Using prediction routine, nodal position and velocity are decided. If any geometrical boundary condition is imposed, they are applied at this stage. With positions of nodes, strain will be decided and stress is available through constitutive law. Integrating stress at Gauss points, internal force at node is available. External force term comes from force boundary condition and difference between the external and internal forces is the bearing force on nodal point. If the difference is divided by nodal mass, then it is acceleration of the node. With new acceleration, velocity is corrected at correction routine. All process is repeated until the given time and results will be picked up at dump frequency.

As shown above, explicit FEM doesn't build any stiffness matrix. Therefore all the calculation is simple compared to implicit one and deformation is simulated along stress wave integration. Detailed explanation on each stage of loop will be given below.

2. Plane strain analysis

Constitutive law for plain strain is explained below. For strain element, rate of deformation has been implemented. Jaumann stress rate is employed in order to remove rigid body motion and rotation. For the simulation loop, nodal points will move as meshes are deformed. Using nodal velocities, velocity gradient is available.

$$\mathbf{L} = \frac{\partial \mathbf{v}}{\partial \mathbf{x}} = \mathbf{D} + \mathbf{W} \quad (1)$$

Velocity gradient is decomposed as rate of deformation \mathbf{D} and spin \mathbf{W} . Rate of deformation is symmetric tensor ($D_{ij} = D_{ji}$) and spin is skew-symmetric tensor ($W_{ij} = -W_{ji}$).

$$\mathbf{D} = \frac{1}{2}(\mathbf{L} + \mathbf{L}^T) \quad (2)$$

$$\mathbf{W} = \frac{1}{2}(\mathbf{L} - \mathbf{L}^T) \quad (3)$$

Using rate of deformation, conventional plane strain constitutive law is applied for stress rate. E is elastic modulus and ν is Poisson constant.

$$\begin{Bmatrix} \dot{\sigma}_{11} \\ \dot{\sigma}_{22} \\ \dot{\sigma}_{12} \end{Bmatrix} = \frac{E}{(1+\nu)(1-2\nu)} \begin{Bmatrix} 1-\nu & \nu & 0 \\ \nu & 1-\nu & 0 \\ 0 & 0 & 1-2\nu \end{Bmatrix} \begin{Bmatrix} D_{11} \\ D_{22} \\ D_{12} \end{Bmatrix} \quad (4)$$

In order to remove rigid body motion, diverse numerical scheme has been developed and several objective rates are favored for large deformation and rotation problems. Among them, Jaumann rate is implemented as shown below.

$$\dot{\sigma}_J = \dot{\sigma} - \mathbf{W} \cdot \sigma - \sigma \cdot \mathbf{W}^T \quad (5)$$

There are other types of objective rates like Truesdell and Green-Naghdi, they will be implemented in future work. Using stress rate, new stress is updated at every loop and Cauchy stress is available for all gauss points.

3. Shape function and Gauss quadrature

Governing equation of FEM analysis is momentum equation and it is given as variational form of principle of virtual work. It is integral equation and would be solved numerically on problem domain. The domain is splitted into sum of grids(meshes). Each mesh has shape functions inside and field variable is approximated using interpolation of shape functions.

$$u \sim \sum_i N_i u_i \quad (6)$$

Shape functions can be any kind of functions which match nodal characteristics but usually linear function is favored. Here, we implemented following linear isoparametric shape function.

$$N_I(\xi) = \frac{1}{4}(1 + \xi_I \xi)(1 + \eta_I \eta) \quad (7)$$

ξ and η are local coordinate. Nodal points (ξ_I, η_I) are shown on Figure 2 and provided below.

$$\begin{Bmatrix} \xi_I \\ \eta_I \end{Bmatrix} = \begin{bmatrix} -1 & 1 & 1 & -1 \\ -1 & -1 & 1 & 1 \end{bmatrix} \quad (8)$$

Momentum equations are integrated numerically using Gauss quadrature. All quadrilateral elements are mapped into local coordinate of Figure 2. After mapping, quad on local coordinate can be integrated using sample points and their weights. We can use one point integration (degenerate element), 4 points, or any other kinds. Conventionally, one point integration with hourglass control is favored but we implemented 4 point integration scheme in order to keep generic methods. This 4 point integration doesn't need hourglass control and is believed to work well on our purpose.

Using Gauss quadrature, spatial integration is done with 4-point (Gauss point).

$$\int \int F(x, y) dx dy = \int_1^1 \int_1^1 f(\xi, \eta) d\xi d\eta = \sum_{i=1}^4 w_i f(\xi_i) \quad (9)$$

$$F(x, y) dx dy = F(x, y) \frac{dx}{d\xi} \frac{dy}{d\eta} d\xi d\eta = F(x, y) |J| d\xi d\eta = f(\xi, \eta) d\xi d\eta \quad (10)$$

If $F(x, y)$ is given as a constant, above equation means just area integration. Jacobian $|J|$ plays an important rule to bridge local and global coordinates. To find Jacobian, we use following matrix relations.

$$\mathbf{J} = \frac{d\mathbf{x}}{d\xi} = \begin{bmatrix} x_{,\xi} & x_{,\eta} \\ y_{,\xi} & y_{,\eta} \end{bmatrix} = \begin{Bmatrix} x_I \\ y_I \end{Bmatrix} [N_{I,\xi}, N_{I,\eta}] = \begin{bmatrix} x_I N_{I,\xi} & x_I N_{I,\eta} \\ y_I N_{I,\xi} & y_I N_{I,\eta} \end{bmatrix} \quad (11)$$

For four node quadrilateral element, there are four global nodal points ($\mathbf{x}_1, \mathbf{x}_2, \mathbf{x}_3, \mathbf{x}_4$)

$$\frac{d\mathbf{x}}{d\xi} = \begin{bmatrix} x_{,\xi} & x_{,\eta} \\ y_{,\xi} & y_{,\eta} \end{bmatrix} = \frac{1}{4} \sum_{I=1}^4 \begin{bmatrix} x_1 \xi_1 (1 + \eta_I \eta) & x_I \eta_I (1 + \xi_I \xi) \\ y_1 \xi_1 (1 + \eta_I \eta) & y_I \eta_I (1 + \xi_I \xi) \end{bmatrix} \quad (12)$$

Using elements of this matrix, Jacobian is estimated.

$$|J| = x_{,\xi} y_{,\eta} - x_{,\eta} y_{,\xi} \quad (13)$$

With inverse matrix of coordinate transfer, inverse relation is also available.

$$\frac{d\xi}{d\mathbf{x}} = \frac{1}{|J|} \begin{bmatrix} y_{,\eta} & -x_{,\eta} \\ -y_{,\xi} & x_{,\xi} \end{bmatrix} \quad (14)$$

For internal force on each node, gradients of shape functions are necessary. On global coordinates derivation could be pain but if we use local coordinate and coordinate transfer,

it can be quite simple. At local coordinate,

$$\frac{\partial N_I}{\partial \xi} = \begin{bmatrix} \frac{\partial N_1}{\partial \xi} & \frac{\partial N_1}{\partial \eta} \\ \frac{\partial N_2}{\partial \xi} & \frac{\partial N_2}{\partial \eta} \\ \frac{\partial N_3}{\partial \xi} & \frac{\partial N_3}{\partial \eta} \\ \frac{\partial N_4}{\partial \xi} & \frac{\partial N_4}{\partial \eta} \end{bmatrix} = \frac{1}{4} \begin{bmatrix} \xi_1(1 + \eta_1\eta) & \eta_1(1 + \xi_1\xi) \\ \xi_2(1 + \eta_2\eta) & \eta_2(1 + \xi_2\xi) \\ \xi_3(1 + \eta_3\eta) & \eta_3(1 + \xi_3\xi) \\ \xi_4(1 + \eta_4\eta) & \eta_4(1 + \xi_4\xi) \end{bmatrix} \quad (15)$$

With inverse relation, gradient of shape function on global coordinate is given as:

$$B_{\mathbf{I}} = \frac{\partial N_{\mathbf{I}}}{\partial \mathbf{x}} = \frac{1}{4} \begin{bmatrix} \xi_1(1 + \eta_1\eta) & \eta_1(1 + \xi_1\xi) \\ \xi_2(1 + \eta_2\eta) & \eta_2(1 + \xi_2\xi) \\ \xi_3(1 + \eta_3\eta) & \eta_3(1 + \xi_3\xi) \\ \xi_4(1 + \eta_4\eta) & \eta_4(1 + \xi_4\xi) \end{bmatrix} \frac{1}{J} \begin{bmatrix} y_{,\eta} & -x_{,\eta} \\ -y_{,\xi} & x_{,\xi} \end{bmatrix} \quad (16)$$

Integrating gradients with stress over domain of element, internal force is calculated.

$$f_{jI}^{int} = \int B_{iI} \sigma_{ij} d\Omega \quad (17)$$

Here, j is a coordinate (x or y), I is a node number, and σ is a stress term. For plane analysis with Updated Lagrangian, above equation can be explained as:

$$f_{xI}^{int} = \int B_{xI} \sigma_{xx} + B_{yI} \sigma_{yx} d\Omega \quad (18)$$

$$f_{yI}^{int} = \int B_{xI} \sigma_{xy} + B_{yI} \sigma_{yy} d\Omega \quad (19)$$

σ_{ij} is Cauchy stress and is available from constitutive law. Above equations can be integrated numerically using Gauss quadrature, and B_{jI} and all stress terms should be estimated at Gauss points of each element beforehand. Integrating on local coordinate, Jacobian is needed and Jacobian term from equation (16) will be vanished.

Assuming constant density, shape functions provides mass allocation of nodes per element. At this stage, we also calculate gradient of shape functions on Gauss points (B_{jI} matrix) and Jacobian at each integration point (= Gauss point). With decided displacement of all nodes, stress at Gauss point is calculated. At constitutive routine, strain is estimated using displacement of all nodes and then stress is updated using conventional plane strain equation.

4. Time integration

We implemented prediction and correction method which is equivalent to velocity Verlet scheme. During time loop, new position and tentative velocity of nodes are calculated (predicted) as shown below.

$$x_{n+1} = x_n + dt \cdot v_n + \frac{1}{2}dt^2 \cdot a_n \quad (20)$$

$$v_{n+\frac{1}{2}} = v_n + \frac{1}{2}dt \cdot a_n \quad (21)$$

After new acceleration is available, velocity term is updated (corrected) using following equation.

$$v_{n+1} = v_{n+\frac{1}{2}} + \frac{1}{2}dt \cdot a_{n+1} \quad (22)$$

C. Postprocessing

After FEM analysis is done, we need to observe and investigate the results. As discussed above, we may use any specialized program for FEM analysis (postprocessing). But we need to consider particle behavior with mesh results, a new program is needed. Hence we made a simple tool which can visualize mesh and particle at the same time.

Using PYTHON and Tkinter library as done in preprocessor, simple visualization program has been built. Basic geometry can be confirmed through this program and some of results like particle temperature and stress at Gauss points are available.

III. MOLECULAR DYNAMICS

Using velocity Verlet scheme, a generic MD has been implemented². To simulate metallic behavior, conventional short-range potential has been practiced for particle-particle interactions. Detailed description of potential can be found at references³⁻⁵. Here we enlist brief review on implemented schemes.

A. Pair potential

For pair potential, we implemented Lennard-Jones (LJ) type potential and modified it at close range in order to converge fast. Conventional LJ potential is given as:

$$\phi_{LJ}(r) = 4\epsilon \left[\left(\frac{\sigma}{r} \right)^{12} - \left(\frac{\sigma}{r} \right)^6 \right] \quad (23)$$

While r_0 is the equilibrium nearest-neighbor separation distance, σ is defined as $r_0/\sqrt[6]{2}$. If particle-particle distance is less than $r_{spl} = 1.244455\sigma$ where is the inflection point of attraction force, equation (23) will be engaged. Otherwise, cubic spline of r^2 is carried out as shown below. If $r > r_{max}$, potential becomes 0 and no force exists between particles.

$$\phi_{spl}(r) = -a_2\epsilon \left[\left(\frac{r_{max}}{\sigma} \right)^2 - \left(\frac{r}{\sigma} \right)^2 \right]^2 + a_3\epsilon \left[\left(\frac{r_{max}}{\sigma} \right)^2 - \left(\frac{r}{\sigma} \right)^2 \right]^3 \quad (24)$$

Using continuity at critical distances like r_{spl} and r_{max} , a_2 is estimated as 0.5424494 and a_3 as 0.09350527 while r_{max} is given as $1.711238\sigma^3$. This truncated LJ potential is presented on Figure 3. We can see that spline curve is continuous and tangential to bare LJ curve but decays faster.

B. Many-body potential

Each pair potential will be implemented as shown above. But it is reported that additional many body potentials - like glue potentials are needed to describe metallic behavior. To do this, we practiced embedded atom method (EAM)^{3,4}. This method measures particle density by searching neighboring particles and develop potential using the density.

$$\rho_i = \sum_{j \neq i} w(r_{ij}) \quad (25)$$

$$w(r_{ij}) = \frac{\rho_0}{d(d+1)} \left[\frac{r_{max}^2 - r_{ij}^2}{r_{max}^2 - r_0^2} \right]^2 \quad (26)$$

ρ_0 is decided as $1/e$ considering equilibrium state⁵. d is dimensional number (2 for 2D and 3 for 3D) and $d(d+1)$ is a coordinate number of FCC structure (6 for 2D, 12 for 3D). e is the base of natural logarithm ($= 2.7182\dots$) and we can define cohesive energy E_{coh} like:

$$E_{coh} = \frac{1}{2}d(d+1)\epsilon \quad (27)$$

Geometric parameters and (111) surface of FCC are illustrated on Figure 4. We can see that EAM include neightorest particles information at equilibrium state. Using those terms, embedding energy function F is provided as shown below.

$$F(\rho_i) = E_{coh} \frac{\rho_i}{\rho_0} \ln \rho_i = \frac{1}{2} d(d+1) \epsilon \frac{\rho_i}{\rho_0} \ln \rho_i \quad (28)$$

Finally, we build inter-atomic potential by combining those pair and EAM potentials.

$$\phi = \chi \phi_{LJ} + (1 - \chi) \phi_{EAM} \quad (29)$$

χ is given as $1/3$. Force equations are available from gradient of potential. They are:

$$-\nabla_x \phi = -\chi \nabla_x \phi_{LJ} - (1 - \chi) \frac{E_{coh}}{\rho_0} (1 + \ln \rho_i) \nabla_x \rho_i \quad (30)$$

$$\nabla_x \rho_i = \sum_{j \neq i} \frac{-4\rho_0 r_{ij}}{d(d+1)} \frac{r_{max}^2 - r_{ij}^2}{(r_{max}^2 - r_0^2)^2} \frac{dr_{ij}}{dx} \quad (31)$$

IV. HOW TO COUPLE FEM AND MD

FEM and MD parts are built respectively. Now problem is how to couple FEM and MD. Let's consider the characteristics of each method and trade-off as shown on Table I. FEM has been developed from civil and mechanical engineering in order to analyze structural problem. Governing equation is momentum equation and force equilibrium on continuum is critical point. Kinetics is main principle and thermodynamic relation is implemented on constitutive law. Therefore it is quite deterministic. Key features are nodal displacements and element stress/strain.

MD is a tool for atomistic scale simulation and has statistical property. Basic behavior is dominated by thermodynamics. Depending on the given potential, particles motions are described in terms of energy and temperature. Particle positions and momenta are fundamental parameters.

As discussed above, bridging between FEM and MD is not continuous. We need some buffer to bridge and communicate for both sides.

A. Direct match of element and particle

We devise the smallest element whose physical size is equivalent to single particle as presented on Figure 5. Effective volume and mass will be exactly same to single particle.

This element is considered as it has a particle inside of element - at the center of element. The center particle will interact with neighboring particles as shown on Figure 6. Then the induced force from particle interaction will be distributed into nodes as provided on Figure 7. On the contrary, if the element is distorted then position change is interpolated and particle position follows. Therefore particle and element can communicate using this method.

The smallest elements are connected into larger ones using coarse graining scheme - those larger ones are combined into more larger ones with same ways. Finally coarse graining will develop until physically meaningful size which can mediate boundary effect.

If any perturbation comes from particles to elements, particles which lie at elements will affect nodal positions and they begin to propagate other FEM field. Using coarse graining elements which sum up small elements into large one, the effect from particles will be summed up into continua - FEM elements. Conversely, stress wave which comes through element can be diffused into neighboring small elements with finer meshes. But this inverse way can induce problems - small elements under coarse element will be under same load by interpolation and this could violate statistical properties. Therefore we need to study more about how to connect them smoothly.

B. Effective particle mapping on element

Second idea is to bind several particles per single element. Those particles will be allocated into single element and averaged property of the particles will be transmitted into the element^{4,6}. Compared to direct match one, this method sums up multiple particles for single element. For broadcasting from element, single element property will be distributed into multiple particles. Therefore we may implement statistical method for the inverse communication. This method will be studied later.

V. EXERCISE

We made a modeling of (111) plane of FCC copper crystal. This plane is composed of uniformly distributed Cu atoms along hexagonal lattice. Lattice constant is 3.61Å and cohesive energy is 3.49 eV/atom. At (111) surface, transverse wave has a speed of (C_{11} -

$C_{12} + C_{44})/3$ while C_{ij} is a stiffness constant⁷. Implemented parameters are provided on Table II.

A. Stress wave transmission

If external forces are imposed on the edge of plane structure which is at free state, stress wave is generated from the edge and crosses whole plane. After reaching the opposite edge, the wave is reflected because it is free edge. The wave crosses whole plane again and reaches free edge again. Therefore stress wave is accumulated on the edges and we can observe continuous increase on edge velocity as shown on Figure 8. With this one dimensional experiment, we can make sure whether MD and FEM modelings are equivalent or not. In addition, any refraction wave can be traced using hybrid model which MD and FEM regions are attached into each other. Figure 9 illustrates basic configurations of each structure. Using parameters of Table II, velocity profile of each method was available. Especially for MD, χ which adjusts between LJ and EAM potential was given as 1 - only LJ potential was used in order to suppress free surface effect which comes from EAM. Figure 10 show their performance - we can make sure initial uprising and amplitude is quite identical. Even though pulse duration and noise on signal show mismatch but it illustrates basic physics is working.

As a refined model, now we suggest a hybrid model as provided on Figure 11. Upper and lower boundaries are FEM elements and we can study wave transmission by changing center body as FEM or MD. Bare FEM model and hybrid structure are indicated on Figure 12. For this experiment, EAM was implemented too. Figure 13 presents the results depending on the method. Overall behavior of each method is consistent but we can find a rise at early stage - even before stress wave is reached if EAM is implemented. The detection point is close to side free surface and it is believed that those early noise comes from free surface effect of EAM. If detection is done at center of free edge then those noise terms will be negligible.

B. Crack propagation

Up to now, we studied linear elastic problems - we may try nonlinear problem which can utilize MD power. We applied similar model which was shown above - but increased MD layer to prevent any nonelastic wave reaching FEM region. Initial configuration is shown on the left of Figure 14. Also artificial crack is implemented at the center of MD layer and we investigated how crack is propagated.

Constant external forces are given on free edge of FEM region and we could see crack propagate along the initial crack as illustrated on the right of Figure 14.

-
- ¹ T. Belytschko, W. K. Liu, and B. Morgan, *Nonlinear Finite Elements for Continua and structures*. John Wiley & sons, LTD, 2000.
 - ² M. P. Allen and D. J. Tildesley, *Computer simulation of liquids*. Oxford Science Publications, 1987.
 - ³ B. L. Holian, A. F. Voter, N. J. Wagner, R. J. Ravelo, S. P. Chen, W. G. Hoover, C. G. Hoover, J. E. Hammerberg, and T. D. Dontje, “Effects of pairwise versus many-body forces on high-stress plastic deformation,” *Physical Review A*, vol. 43, no. 6, pp. 2655–2661, 1991.
 - ⁴ W. G. Hoover, A. J. D. Groot, and C. G. Hoover, “Massively parallel computer simulation of plane-strain elastic-plastic flow via nonequilibrium molecular dynamics and Lagrangian continuum mechanics,” *Computers in physics*, vol. 6, no. 2, pp. 155–167, 1992.
 - ⁵ B. L. Holian and R. Ravelo, “Fracture simulations using large-scale molecular dynamics,” *Physical Review B*, vol. 51, no. 17, pp. 11275–11288, 1995.
 - ⁶ S. P. Xiao and T. Belytschko, “A bridging domain method for coupling continua with molecular dynamics,” *Computer methods in applied mechanics and engineering*, vol. 193, pp. 1645–1669, 2004.
 - ⁷ C. Kittel, *Introduction to solid state physics*. Wiley, 1996.

TABLE I: Comparison for FEM and MD

Method	FEM	MD
attribute	deterministic	statistical
dominance	kinetics	thermodynamics
force parameter	stress	momentum
spatial parameter	strain	position

TABLE II: Simulation parameters for Cu (111) surface

property	value	unit
elastic modulus	44.367	GPa
poisson ratio	0.34	-
density	9,018	kg/m ³
cohesive energy	3.49	eV
atomic mass	63.55	a.m.u.
NN distance	2.553	Å

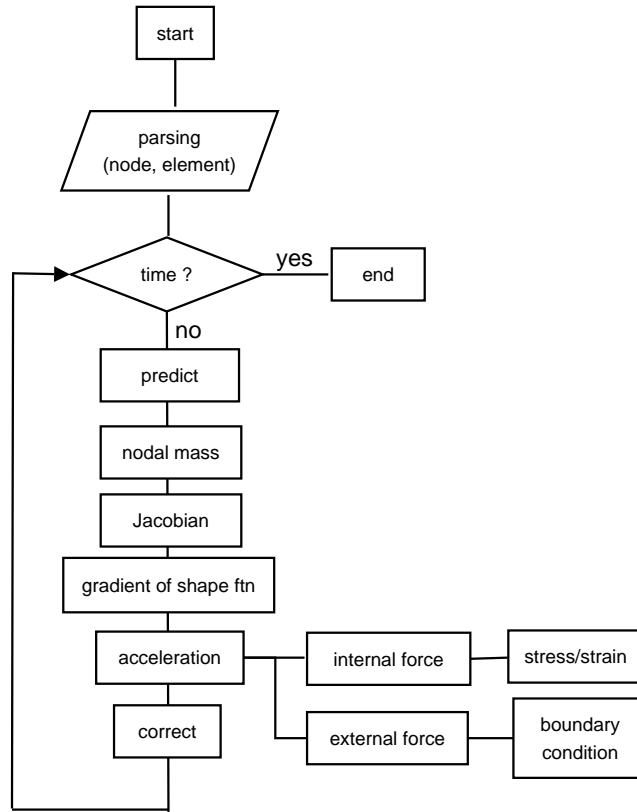


FIG. 1: Flow chart of explicit FEM analysis

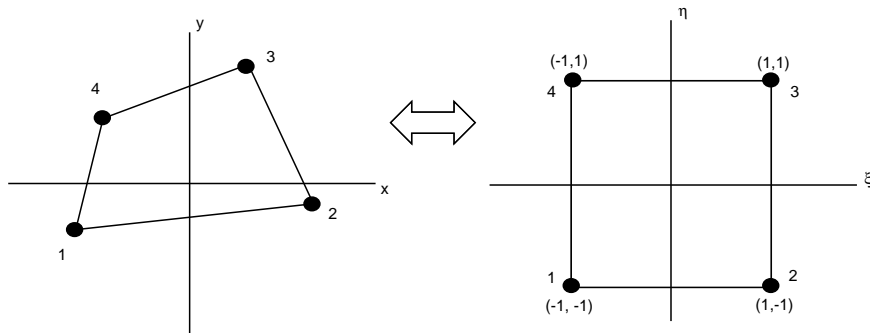


FIG. 2: Global and local coordinate systems

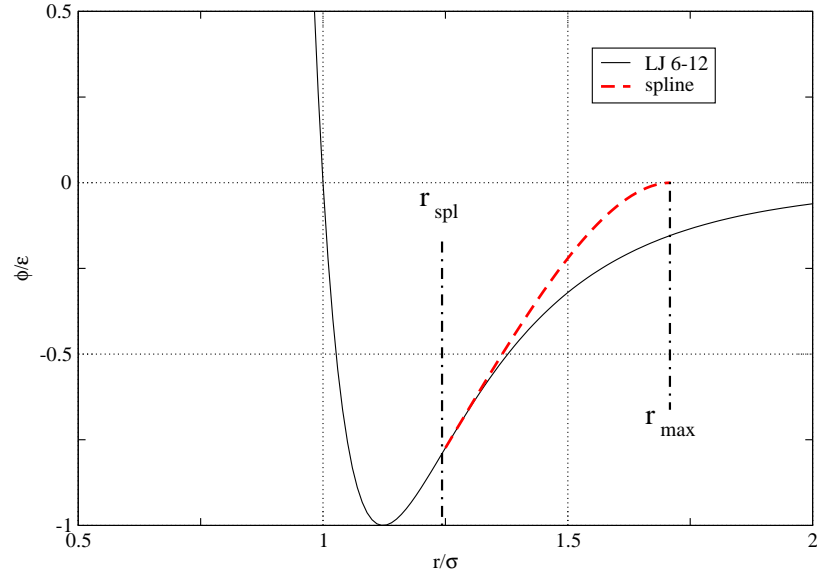


FIG. 3: LJ potential and modified spline curve

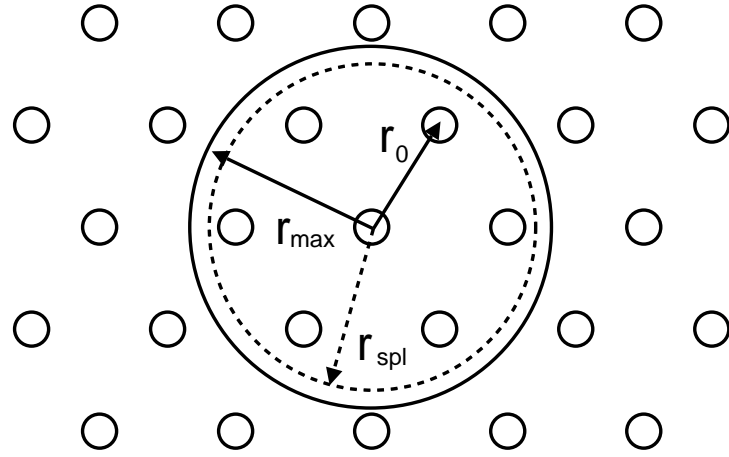


FIG. 4: Radii of EAM parameters and neighboring particles at (111) surface of FCC structure



FIG. 5: Direct coupling of elements and particles

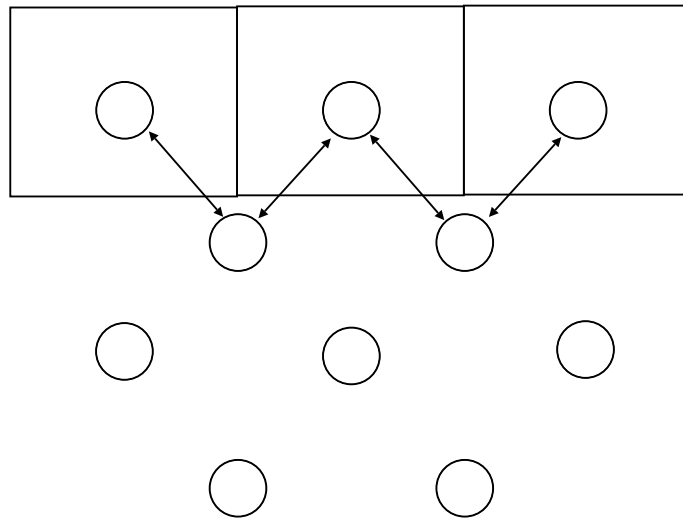


FIG. 6: Particle interactions between coupled and independent ones

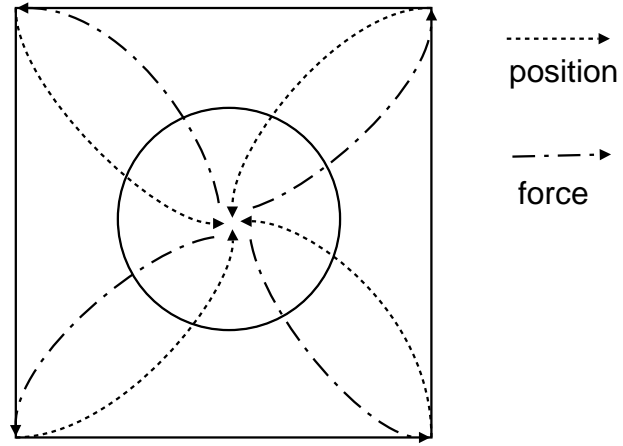


FIG. 7: Position interpolation and force distribution between coupled particle and element

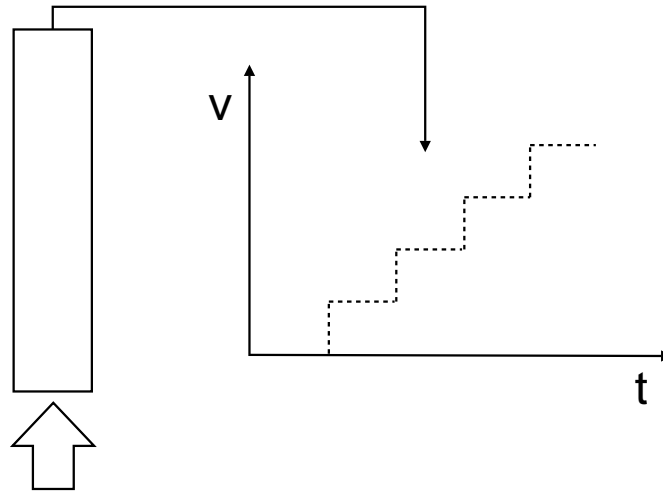


FIG. 8: Modeling for one-dimensional wave propagation experiment

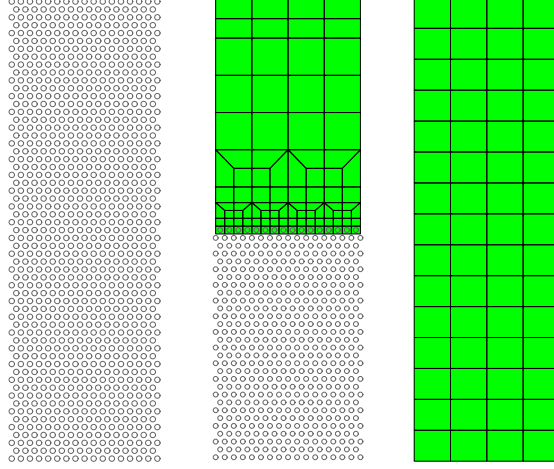


FIG. 9: Bare MD (left), hybrid (middle), and FEM (right) structures for 1-D stress wave propagation experiment

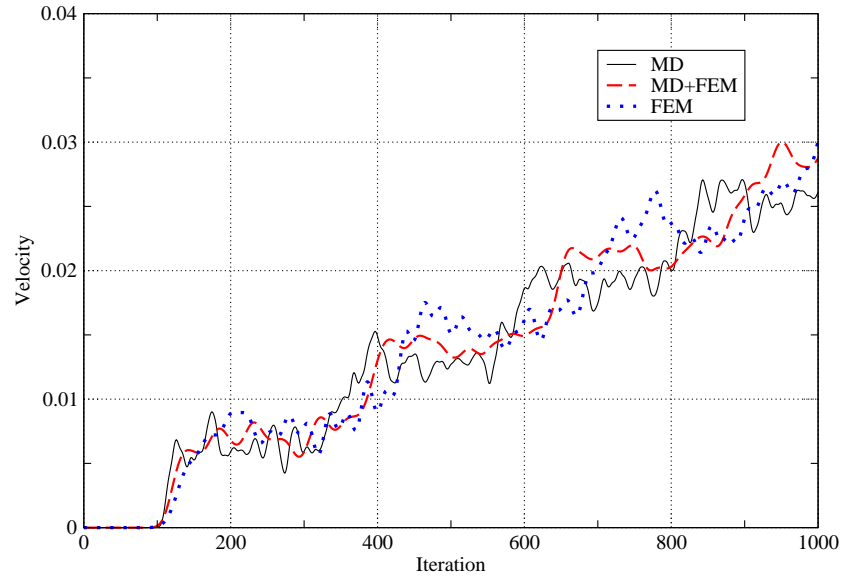


FIG. 10: Velocity profile of end edge for 1-D stress wave simulation

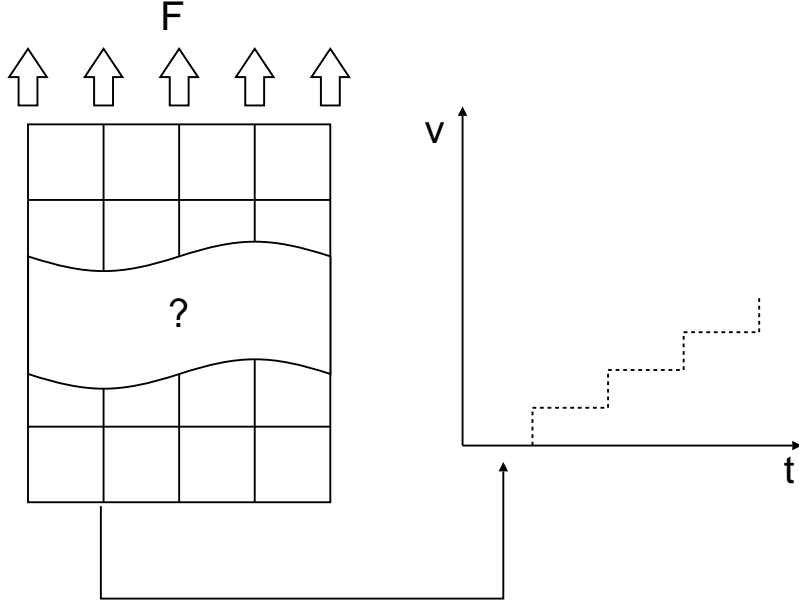


FIG. 11: Stress wave propagation experiment for hybrid structure

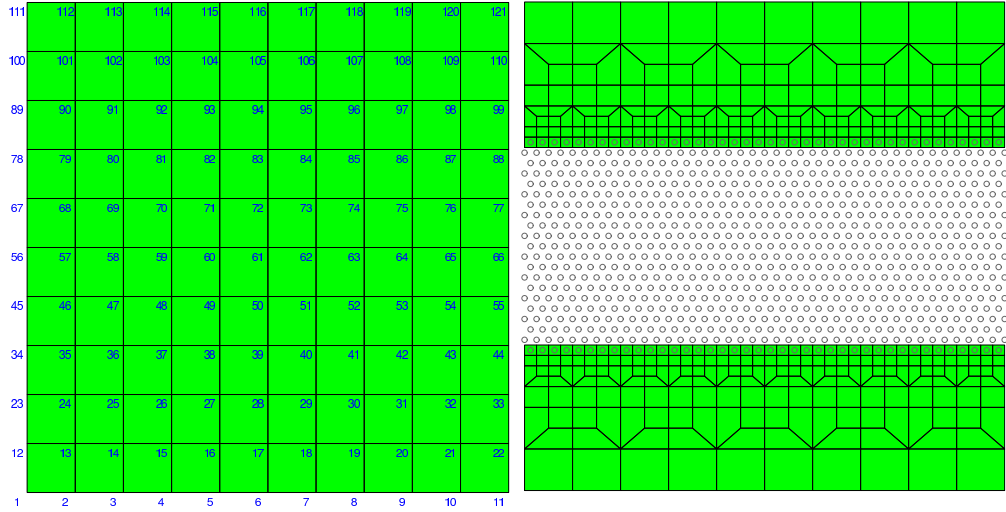


FIG. 12: Bare FEM (left) and hybrid (right) structures for stress wave propagation

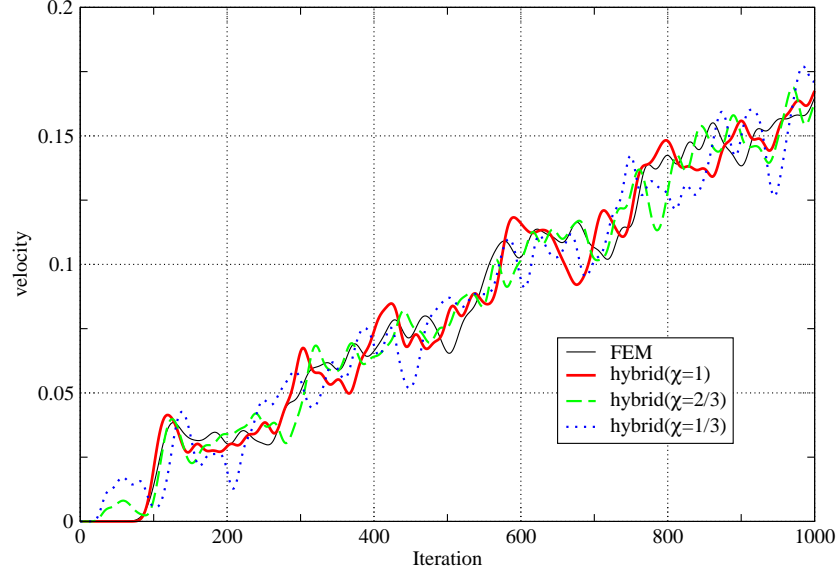


FIG. 13: Stress wave propagation results for hybrid and bare FEM structures

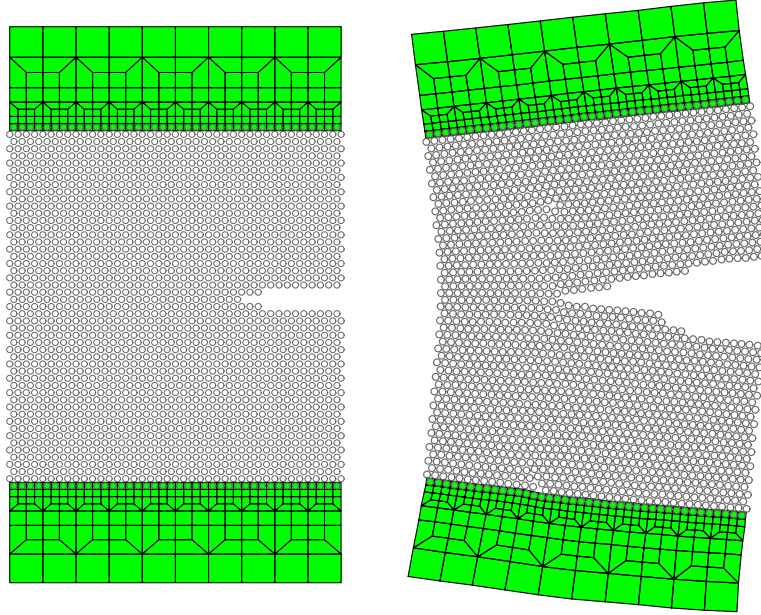


FIG. 14: Initial configuration (left) and intermediate result (right) of FEM and MD analysis for crack propagation